Thus the proposed method for calculating flows of composite jets permits finding, aside from the value of x_a, the characteristics of the flow in intermediate sections and their limiting values, making it possible to study later the stability of the given flow.

In conclusion we note that the method can be extended to the case of a multilayer jet, but the larger number of implicit linear differential equations in this case for determining the x derivatives as a function of the ordinates of the interface surfaces makes it necessary to execute the approximation algorithm repeatedly for a fixed value of x; this substantially increases the computing time.

LITERATURE CITED

1. C. H. Hertz and B. Hermanrud, "A liquid compound jet," J. Fluid Mech., 131, 271 (1983).
2. S. Radev and P. Gospodinov, "Numerical treatment of the steady flow of a liquid compound jet," Int. J. Multiphase Flow, 12, No. 6 (1986).
3. V. Ya. Shkadov, Some Methods and Problems in the Theory of Hydrodynamic Stability [in Russian], Moscow State University Press, Moscow (1973).
4. V. E. Epikhin and V. Ya. Shkadov, "Flow and instability of capillary jets interacting with the surrounding medium," Izv. Akad. Nauk SSSR, Mekh. Zhidk. Gaza, No. 6 (1978).
5. G. M. Sisoev, A. F. Tal'drik, and V. Ya. Shkadov, "Flow of a film of viscous liquid along the surface of a rotating disk," Inzh.-Fiz. Zh., 51, No. 4 (1986).
6. D. Gottlieb and S. A. Orszag, Numerical Analysis of Spectral Methods: Theory and Applications, Philadelphia (1977).
7. S. Pashkovskii, Applications of Chebyshev Polynomials and Series in Computing [in Russian], Nauka, Moscow (1983).
8. N. N. Kalitkin, Numerical Methods [in Russian], Nauka, Moscow (1978).

INVESTIGATION OF NATURAL CONVECTION AND CONVECTION STIMULATED BY LOCAL IRRADIATION IN A THIN LAYER OF EVAPORATING LIQUID

V. V. Nizovtsev

UDC 532.516:772.96

Capillary convection in low-viscosity liquids is observed with surface-tension differentials of the order of 0.1 mN/m. It appears in many technological processes. Convection leading to the formation of a relief on the boundary of the interface arises in a layer of drying paint and varnish or glassy enamel as well as accompanying extraction in liquid—liquid systems or rectification of multicomponent mixtures [1-4]. Fluctuational surface-tension gradients initiate convection.

The high sensitivity of liquids to shear stresses has been employed to solve technical problems, such as separation of impurities [5], obtaining relief photographic images [6, 7], deposition of matter at a fixed location of a substrate [8], or surface doping of metals [9]. The technical solutions listed are based on capillary convection, controlled by the thermal action of radiation [10, 11]. In spite of the wide range of possible applications of forced capillary convection virtually no quantitative data on convection under the action of radiation and its comparison with spontaneous convective processes have been published. The results of a study of capillary-convective instability of a layer of liquid in the regime of natural evaporation and under conditions of local heating by low-power laser radiation are presented below.

1. Materials and Methods. Convection in solutions of crystal violet dye in polar organic solvents was studied (see Table 1). The dye contrasted the image of the relief on the surface of the layer and simultaneously functioned as a strain-active and light-absorbing additive. Thermal capillary convection was induced by the action of a Gaussian beam of

Moscow. Translated from Zhurnal Prikladnoi Mekhaniki i Tekhnicheskoi Fiziki, No. 1, pp. 138-145, January-February, 1989. Original article submitted October 12, 1987.

0021-8944/89/3001-0132$12.50

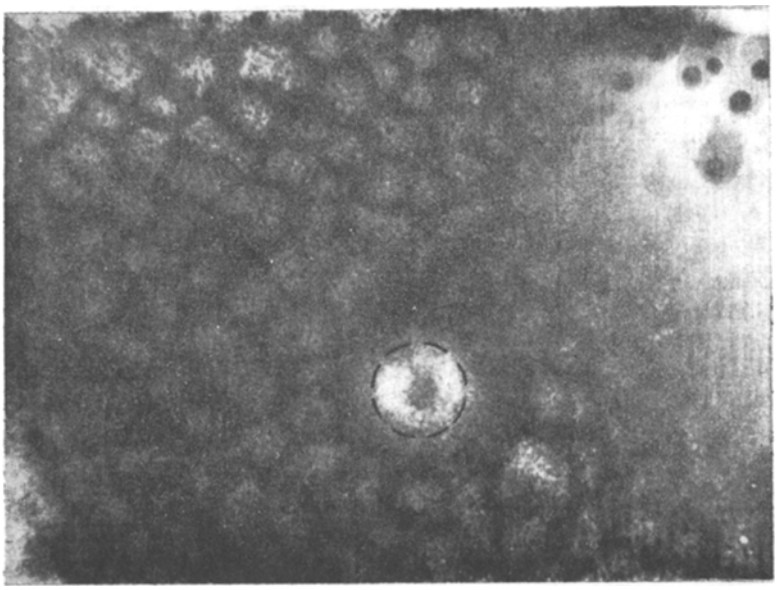

Fig. 1

radiation from a 1 mW helium—neon laser with a beam diameter in the plane of the layer ranging from 0.8 to 2.4 mm. The dye concentration of about 10 g/liter was chosen so as to achieve near 633 nm unit optical density in a layer not greater than 0.1 mm thick. Layers from 0.1 to 1.0 mm thick were deposited on a polymethyl methacrylate substrate (PMMA), silicate glass, or brass with thermal conductivities of 0.2, 1.0, and 100 W/(m·K), respectively. The velocity of the liquid particles on the surface and the size of the convective cell were determined with the help of motion pictures and photographs, made in reflective light, of a layer of lycopodium powder suspension in the solution. The lycopodium particles traced the streamlines of the liquid. The reflief on the surface of the layer was determined by microphotometric measurements of the photographic image of the layer, obtained in transmitted light.

2. Spontaneous Convection Cells in an Evaporating Layer. In the regime of natural convection, like under the action of radiation, it may be expected that convection of a temperature and concentration nature will appear, since the surface tension σ depends on both the temperature and the concentration of the solution. The difference $\delta\sigma$ in the surface tension between sections of the surface layer with different temperature T and concentration C equals

$$\delta\sigma = \sigma_T'\delta T + \sigma_C'\delta C = \delta\sigma_T + \delta\sigma_C. \tag{2.1}$$

Here σ_T' and σ_C' are the average coefficients of the temperature and concentration dependences of the surface tension. For the solutions studied $\sigma_T' \approx -0.1$ mN/(m·K), $\sigma_C' \approx 0.1$ N·liter/(m·kg) [14].

As the solvent evaporates the temperature decreases and the concentration of the solution at the surface increases. Calculations for ethyl alcohol on silicate glass, performed by the method of [15], gave a temperature difference between the bottom and free surface of the liquid layer of about 15°K. In the calculation it was assumed that mixing of the liquid does not occur and that the temperature of the lower boundary of the layer is the same as that of the surrounding medium, since it is in thermal contact with the glass, whose thermal conductivity is many times higher than that of alcohol. Under real conditions the temperature difference is smaller owing to convection in the layer, but, being a consequence of continuous evaporation and the reason for the convection itself, this difference is always positive. In addition to a temperature gradient, there also exist in the layer a transverse concentration gradient, owing to the evaporation of solvent from the surface. Thus under the conditions of evaporation the layer is in a state with excess surface energy, since liquid with a higher surface tension than in the bulk of the layer is located near the open interphase boundary. This state is unstable and leads to the formation of circulation convective flows, deforming the surface.

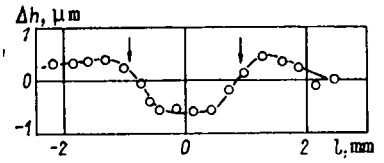

Fig. 2

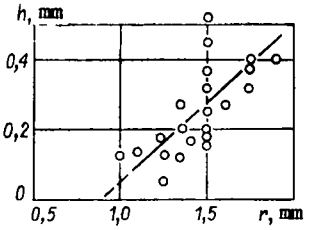

Fig. 3

Cells in the evaporating layer can be observed only in the absence of spreading; we achieved this by depositing the layer on a substrate consisting of a circular piece of glass with a diameter of about 2 cm. The sharp edge of the substrate confined the liquid within the glass, preventing the spreading ordinarily present in such cases [14] or creeping onto the wall of the cell [16]. Figure 1 shows a picture of a section of a layer of butanol 0.3 mm thick 2 min after the solution was deposited on the glass. The light-colored sections correspond to depressions on the surface of the layer. The cells have a polygonal and unstable shape, since weak but constant centrifugal transport of matter occurs along the layer and accumulation of matter at the periphery of the substrate owing to axisymmetric surface temperature and concentration gradients [17]. The most significant and stable convection cells are formed in layers of liquids from the middle of the table. Cells with a spacing of 0.9 ± 0.1 mm appeared after 2-3 min in a layer of butanol solution 0.3 ± 0.03 mm thick. For the more volatile ethanol the cell-formation time is about 1 min, and the cell spacing in a layer 0.15 ± 0.03 mm thick equalled 0.4 ± 0.1 mm. The cell spacing is always approximately three times greater than the thickness of the layer, which is true in general for cells of this type [18]. Microphotometric measurements show that the depth of the relief above spontaneous cells does not exceed 0.5 μm. At the final stages of evaporation of the solvent the cells decomposed owing to convection, accompanying drying [14].

3. Convection Accompanying Local Irradiation. Under irradiation different types of convection, depending on the ratio of the absolute values of the terms in (2.1), can be observed. For $|\delta\sigma_T| > |\delta\sigma_C|$ solution flows out of the irradiated section, while for the opposite inequality the film of solution flows into the irradiated zone of the layer owing to concentration convection. The phenomenology of the second case is studied in [8, 19].

The first situation is realized at the start of irradiation and remains for many minutes in the case of layers greater than 0.3 mm thick, where the concentration of the solution in the irradiated zone does not increase, so that $\delta C \approx 0$, and hence $\delta\sigma \approx \delta\sigma_T < 0$. Decreasing the surface tension leads to the appearance of centrifugal surface flows, which, owing to the finite viscosity of the liquid, form a relief in the form of a depression surrounded by a ridge. The difference of the capillary pressures between the toroidal zone of the ridge and the center of the irradiated section of the surface gives rise to reverse flows in the lower part of the layer. In the stationary state the mass transport by contradirectional flows is balanced and a convection cell with stationary velocity and temperature distributions and surface profile forms. Figure 2 shows the axial section of the depression for a 0.3 mm thick layer of solution in butanol on glass. The arrows mark the boundaries of the beam, and l is the distance from its axis. The asymmetric character of the profile is due to the surface convection in the layer, which cannot be completely suppressed. In this connection, as well as because of the neighboring spontaneously arising evaporation cells, additionally deforming the surface, the position of the undisturbed surface of the liquid (zero line) in Fig. 2 is somewhat arbitrary.

The radius r of the cell is virtually independent of the viscosity and is determined primarily by the thickness of the layer h and the diameter of the radiation beam. In Fig. 3 the straight line corresponds to a beam with a radius of 0.9 mm. The boundary of the beam is determined based on radiation intensity of 0.1 of the maximum value. This criterion was chosen, in particular, based on the fact that in this case as the thickness of the layer approaches zero the radius of the cell approaches the radius of the beam. It is important to note that for low radiation power the diameter of the cell is virtually independent of the thermal conductivity of the substrate and the power supplied. Thus with a beam radius of 0.4 mm reducing the power by a factor of five reduces the size of the cell by only 20%. The cell sizes are the same, to within 20%, for all substrate materials. The spread of the

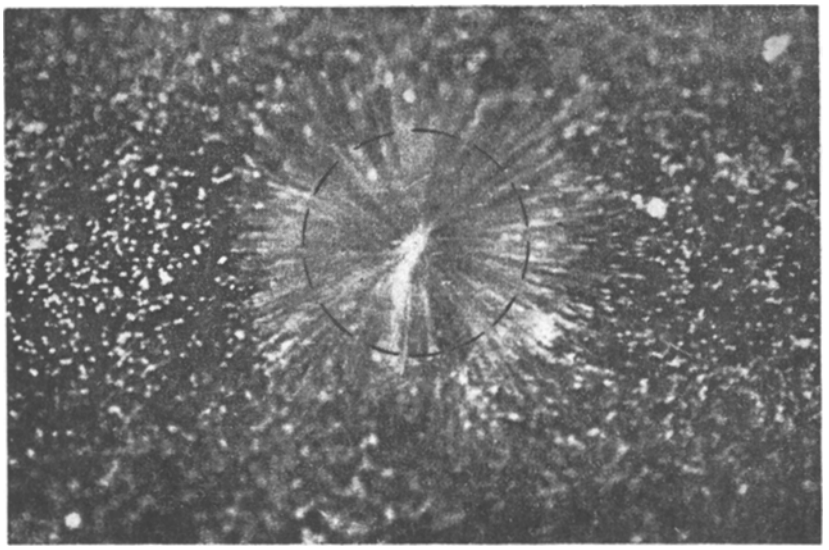

Fig. 4

experimental points in Fig. 3 is due to the low accuracy of the measurements of both the thickness of the unstable layer and the size of the section of the layer encompassed by convection. In photographs of the images the boundary of the cell cannot always be determined accurately enough (Fig. 4). It is interesting to compare the ratio of the thickness of the layer and the radius of the cell (Fig. 3) with the same ratio for spontaneous cells. It was noted above that under conditions of evaporation convection in thin layers the radius of the cell is about 1.5h. In the case of forced convection for thicknesses from 0.1 to 0.5 mm the linear approximation of the scattering diagrams $r = r_b + 1.5h$, where r_b is the radius of the beam and the coefficient in front of h has an rms deviation of 0.3.

The cell created by local irradiation affects the arrangement of neighboring cells, leaving their spacing unchanged (see Fig. 1). The broken lines on the photograph denote the zone of irradiation with a diameter of 1.8 mm. The picture was made after repeated duplication of the starting negative, as a result of which the contrast of the image increased at the expense of some loss of resolution.

4. Mass Transfer under Conditions of Convection. Table 1 gives the experimental values of the velocity v_s of the liquid on the surface of the cell at a point corresponding to the inflection on the lateral wall of the depression for a layer 0.35 mm thick on glass. Decreasing the power by a factor of five leads to an approximately five-fold decrease in the velocity. For butanol with a thickness of 0.15 mm, $v_s = 0.9 \pm 0.2$ mm/sec. Increasing the viscosity and decreasing the thickness of the layer have a negative effect on the rate of convection.

Direct observations showed that vertical motion at the center of the cell occurs in a very narrow channel. For a beam about 2 mm in diameter the channel has a diameter of about 0.2 mm. Thus the total length of the horizontal section of the convective path can be set equal to r. To evaluate the velocity on the surface of the layer we shall assume that in the transverse section of the convection cycle a linear vertical distribution of the velocity in centrifugal flow and a parabolic distribution in the reverse flow are observed under the point of inflection at a distance equal approximately to r/2 from the axis of the beam [20]. A flow of the latter type is driven by the pressure difference $p_2 - p_1$ in the peripheral and central regions of the cell. In addition, the velocities equal zero on the substrate and at a height $2a$ above the substrate. We shall place the origin of the vertical z axis at a height a above the substrate. Then

$$v_1 = B(z - a),\ a \leqslant z \leqslant h - a; \tag{4.1}$$

$$v_2 = -\frac{a^2[1-(z/a)^2]}{2\mu}\frac{(p_2 - p_1)}{b},\ |z| \leqslant a. \tag{4.2}$$

Here v_1 and v_2 are the velocities of the centrifugal and reverse flows; b is the distance between the central meniscus (the depression itself) and the meniscus of the ridge, or the

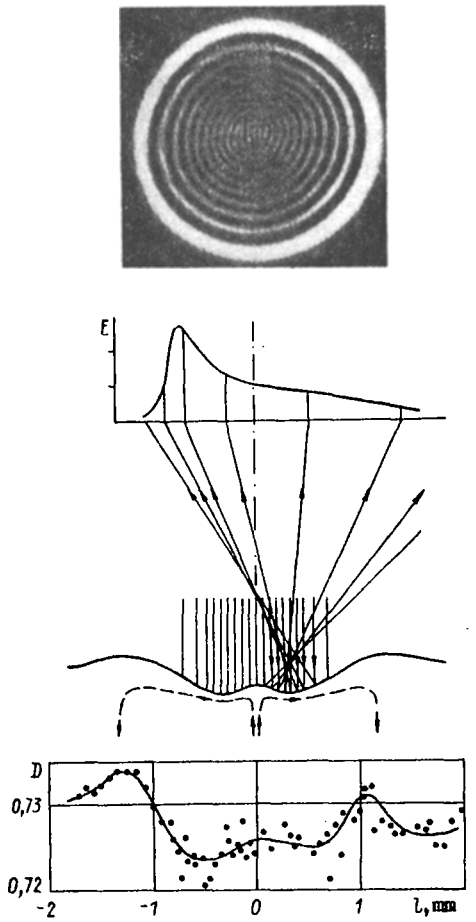

Fig. 5

radius of the torus, approximately equal to r; B is a constant. The reverse flow under the point of inflection on the surface of the layer is due to the average gradient of the Laplacian pressure: $(p_2 - p_1)/b \approx (\sigma/r)(1/R_2 + 2/R_1)$ (R_2 and R_1 are the average radii of curvature of the toroidal ridge and the depression at the center).

For the studied thicknesses of the layer the gravitational convection can be neglected, since the static Bond number, defined as the ratio of the hydrostatic forces to the capillary forces, does not exceed 0.1. Cline [21] also arrived at the conclusion that capillary forces play the predominant role in laser processing of the surface of a metal.

From the conditions of joining of the derivatives of the functions (4.1) and (4.2) at the point a it follows that $B = (a\sigma/r\mu)(2/R_1 + 1/R_2)$. Based on the fact that the volume flow rates in centrifugal and reverse flows are equal we obtain analogously to [22] $a = h/3$. The velocity v_s of particles on the surface of the layer is found from the expression

$$v_s = (h^2\sigma/(9r\mu))(2/R_1 + 1/R_2). \qquad (4.3)$$

The radii R were determined from graphs analogous to Fig. 2. Based on the reasons mentioned in Sec. 3, the relative error in this case equalled about 30%. For butanol with thicknesses of 0.25 and 0.35 mm the average radii of curvature are equal and constitute about 0.5 m. The expression (4.3) gives velocities of 0.25 and 0.5 mm/sec, respectively. The computed values are close to the experimental values, equal to 0.3 ± 0.1 and 2.0 ± 0.5 mm/sec, respectively.

Direct observations and calculations indicate that on straight sections of the convection path the flow is laminar. Even for liquids with low viscosity, for which the velocity on the surface is of the order of 10 mm/sec, Reynolds number Re does not exceed 2 for a centrifugal flow and 25 for the vertical tube at the center of the cell; for a centrifugal flow $Re = av_s\rho/\mu$. In evaluating Re for the vertical flow the velocity was calculated starting from the assumption that the volume flow rates in a central cylindrical channel 0.2 mm in

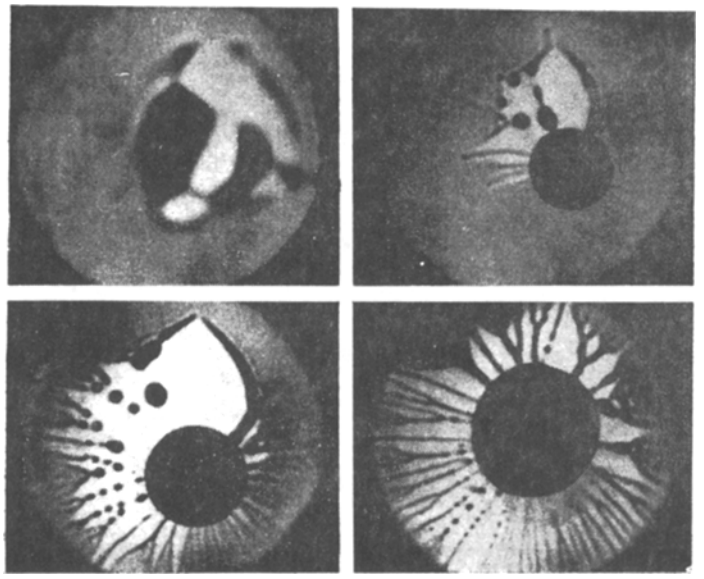

Fig. 6

diameter equals that in the reverse flow at a distance r/2 from the center. Since $a = h/3$ the average velocity of the reverse flow was assume to be equal to $v_s/4$; then it equals about 60 mm/sec in the vertical channel.

5. Relief at the Bottom of the Depression. The distribution of the radiation in the cross section of the beam reflected by the depression is shown at the top of Fig. 5. The distribution was obtained at a height of 1 m above the layer; the diameter of the outer ring equals 15 mm. The pattern obviously originates from interference. This question was studied theoretically in [23], but experimentally it has been studied only qualitatively. It was proposed in [23, 24] that the pattern obtained is the result of interference of beams reflected by the depression itself and the convex toroidal mirror of the ridge around it. Figure 2, however, shows that the toroidal ridge cannot be manifested in the interference pattern, since it falls outside the radiation beam.

Microphotometric measurements of the images of the deformed section of the surface, obtained after duplication and increasing the contrast, revealed a pronounced convexity at the center of the depression. Figure 5 shows a microphotogram of the double-positive of the image of the cell, whose profile is shown in Fig. 2. As one can see, on the whole, the relief on the surface of the layer has the form of a bowl. At the center of the deformed section of the surface the direction of motion of the particles of the liquid changes abruptly from vertically upwards to horizontal (shown by the broken lines). The hydrodynamic pressure of the stopped jet is balanced by the Laplacian pressure of the convex meniscus. The reconstruction of the surface profile from the microphotogram and the expected distribution of illumination E in the cross section of the beam reflected from one side of the profile are presented at the center of Fig. 5. The interference of such distributions gives the pattern shown at the top of Fig. 5. The divergence of the reflected beams and, therefore, the diameter of the interference pattern are determined by the curvature of the toroidal trough at the bottom of the depression. For this reason it increases as the thickness of the layer decreases (as the walls of the depression are approached) and as the radiation power is increased or the thermal conductivity of the substrate is increased (the rate of convection is increased).

6. Formation of a Convection Cell. The development of convection was studied by analyzing the changes in the geometry of the beam reflected by the depression. The behavior of the diameter of the interference pattern is determined by the change in the curvature of the surface layer and hence reflects the dynamics of formation of the cell. The distance from the layer to the cell was chosen to be quite large ($\sim$3 m), so that on it the reflected beam would be diverging for a large fraction of the formation time of the cell. Table 1 gives the values of the rate constant k for the formation of cells in layers 0.3 mm thick on glass. In the case of butanol constants are presented for a layer on PMMA, glass, and brass,

TABLE 1

Solvent	μ, 10^{-3} Pa·sec (temperature, °C) [12]	σ, mN/m	σ'_T, mN/(m·K) [13]	v_s, mm/sec	k, sec^{-1}
Acetone	0,32 (20)	23,7	—0,11	—	—
1,2-Dichloroethane	0,80 (25)	32,5	—0,14	—	—
Ethanol	1,08 (25)	22,8	—0,08	4,8±1,6	3,1
Butanol	2,95 (20)	24,6	—0,09	2,0±0,5	1,7; 2,5; 3,6
Octanol	7,6 (25)	27,5	—0,08	0,5±0,2	1,8
Cyclohexanol	68 (20)	26,5	—0,10	0,25±0,05	2,0

respectively. In analyzing the data we assumed that the diameter Φ of the pattern changes with time t according to the law

$$\Phi = \Phi_s[1 - \exp(-kt)] \tag{6.1}$$

(Φ_s is the stationary value of the diameter). The results were usually described well by the expression (6.1) right up to the values $\Phi = 0.8\Phi_s$, after which the process slowed down somewhat. It follows from the table that the time at which the stationary state is achieved is virtually independent of the viscosity of the liquid and the thermal conductivity of the substrate.

For a thin layer and a volatile solvent the development of thermocapillary convection is complicated by the evaporation of liquid. For a layer 0.2 mm thick on PMMA and a power of 1 mW after 20 sec of irradiation the layer bursts owing to the accumulation of heat, intensification of convection, and evaporation of the solvent. In the process the character of the convection changes from thermocapillary to concentration convection, since the absolute value of the second term in the expression (2.1) becomes greater than that of the first term. At the center of the irradiated zone a drop of concentrate collects on the exposed substrate; the drop absorbs radiation energy and an axisymmetric temperature gradient is created around it on the substrate. This temperature gradient maintains centripetal flow of liquid to the drop in the form of streams and small drops. Figure 6 shows the development of concentration convection after the bursting of a layer on an irradiated section 0.6 mm in diameter. For a small volume of the gas phase and prolonged irradiation dissolved matter accumulates at the center of the irradiated zone, and pure solvent remains on the cold sections of the substrate [5, 19].

I thank G. P. Lur'e for assistance in performing the studies.

LITERATURE CITED

1. J. N. Anand and R. Z. Balwinsky, "Surface deformation of thin coatings caused evaporative convection," J. Colloid Interface Sci., 31, No. 2 (1969).
2. A. D. Yakovlev, Chemistry and Technology of Paint and Varnish Coatings [in Russian], Khimiya, Leningrad (1981).
3. M. V. Ostrovskii, "On the appearance of large-scale pulsating cellular convection on a phase interface with extraction in liquid—liquid systems," Kolloid. Zh., 38, No. 5 (1976).
4. I. A. Aleksandrov, Mass Transfer Under Conditions of Rectification and Absorption of Multicomponent Mixtures [in Russian], Khimiya, Leningrad (1975).
5. B. A. Bezuglyi, E. A. Galashin, et al., "Separation of impurities in a liquid under the thermal action of laser radiation," Pis'ma Zh. Tekh. Fiz., 2, No. 18 (1976).
6. B. A. Bezuglyi and E. A. Galashin, "Thermal strain micrography — a new method for obtaining images," Zh. Nauch. Prikl. Fotogr. Kinematogr., 27, No. 1 (1982).
7. B. A. Bezuglyi, N. P. Netesova, and V. V. Nizovtsev, "X-ray diffraction photosensitive material," Inventor's Certificate No. 1113774, SSSR; Byull. Izobr., No. 34 (1984).
8. B. A. Bezuglyi, E. A. Galashin, and A. N. Fedotov, "Investigation of photocondensation and photocrystallization phenomena," Zh. Nauch. Prikl. Fotogr. Kinematogr., 22, No. 1 (1977).
9. I. B. Borovskii, D. D. Gorodskii, et al., "Surface doping of metals with the help of continuous laser radiation," Fiz. Khim. Obrab. Mater., No. 1 (1984).

10. B. A. Bezuglyi, "Capillary convection controlled by the thermal action of light and its application in information recording methods," Author's Abstract of Candidate's Dissertation in Physical-Mathematical Sciences, Moscow State University, Moscow (1985).
11. A. T. Sukhodol'skii, "Photocapillary phenomena," Izv. Akad. Nauk SSSR, Ser. Fiz., 50, No. 6 (1986).
12. N. B. Vargaftik, Handbook of the Thermophysical Properties of Gases and Liquids [in Russian], Nauka, Moscow (1972).
13. A. A. Abramzon and E. D. Shchukin (eds.), Handbook of Surface Phenomena and Surfactants [in Russian], Khimiya, Leningrad (1984).
14. V. V. Nizovtsev and N. P. Netesova, "On the spreading of a drop of ethanol solution of crystal violet," Kolloid. Zh., 47, No. 5 (1985).
15. N. A. Fuks, Vaporization and Growth of Drops in a Gaseous Medium [in Russian], USSR Academy of Sciences Press, Moscow (1958).
16. A. F. Pshenichnikov and G. A. Tokmenina, "Deformation of the free surface of a liquid by thermocapillary motion," Izv. Akad. Nauk SSSR, MZhG, No. 3 (1983).
17. V. V. Nizovtsev and N. P. Netesova, "Capillary convection accompanying spreading and vaporization of a drop of surfactant solution," Kolloid. Zh., 47, No. 6 (1985).
18. D. Joseph, Stability of Fluid Motion, Springer-Verlag (1976).
19. B. A. Bezuglyi and V. V. Nizovtsev, "Study of the formation of drops accompanying irradiation of capillary films of solutions with light," Vestn. MGU. Ser. 3, Fizika, Astronomiya, 22, No. 6 (1981).
20. R. Bird, V. Stewart, and E. Lightfoot, Transport Phenomena [Russian translation], Khimiya, Moscow (1974).
21. H. E. Cline, "Surface rippling induced in thin film by a scanning laser," J. Appl. Phys., 52, No. 1 (1981).
22. Yu. V. Sanochkin, "Steady thermocapillary motion in a horizontal layer of liquid metal heated locally from above," Izv. Akad. Nauk SSSR, Mekh. Zhidk. Gaza, No. 6 (1984).
23. G. da Costa and J. Calatroni, "Transient deformation of liquid surface by laser-induced thermocapillarity," Appl. Opt., 18, No. 2 (1979).
24. G. da Costa, "Thermocapillary self-focusing of a laser beam," Phys. Lett., 80a, No. 4 (1980).

DEVELOPMENT OF THERMOGRAVITATIONAL CONVECTION IN THE PRESENCE OF SOLUBLE SURFACE-ACTIVE MATTER AT THE INTERFACE

A. A. Nepomnyashchii and I. B. Simanovskii

UDC 536.25

The effect of insoluble surface-active matter (SAM), deposited on the interface, on the development of thermogravitational convection in a two-layer system was investigated in [1], where a new type of oscillatory instability of the equilibrium was detected.

The present article explores the effect of SAM solubility on the monotonic and oscillatory modes of instability. It has been found that an increase in SAM solubility lowers the monotonic instability threshold and narrows the range of parameters where oscillatory instability is more critical.

Assume that the space between two solid horizontal plates, which are maintained at different constant temperatures (the temperature difference is θ), is filled with two viscous, immiscible mediums. The coordinate origin is located at the interface, the x axis is horizontal, and the y axis points vertically upward. The equations of the solid boundaries are $y = a_1$ and $y = -a_2$. The coefficients of dynamic and kinematic viscosity, thermal conductivity, thermal diffusivity, and volume expansion are η_m, ν_m, $\varkappa_m$, χ_m, and β_m, respectively ($m = 1$ for the top layer and $m = 2$ for the bottom layer). The effect of distortion of the interface is neglected, and the interface is assumed to be flat and nondeformable ($y = 0$).

Perm'. Translated from Zhurnal Prikladnoi Mekhaniki i Tekhnicheskoi Fiziki, No. 1, pp. 146-149, January-February, 1989. Original article submitted October 10, 1987.

